JOURNAL OF MATERIALS SCIENCE **37** (2002) 295–301

Viscoelastic properties of polymer films on surface acoustic wave organophosphorous vapor sensors

CHI-YEN SHEN
Department of Electrical Engineering, I-Shou University, Kaohsiung County 840, ROC
YU-TANG SHEN, LONG WU
Department of Electrical Engineering, National Cheng Kung University, Tainan, 701, ROC

This work investigates the viscoelastic properties of the fluoropolyol (FPOL) polymer on the surface acoustic wave (SAW) organophosphorous vapor sensors. A complex shear modulus is used to express different polymer types (glassy, glassy-rubbery, and rubbery). The different polymer types leads to different propagating properties of SAW, such as attenuation change and velocity shift. Calculation results indicate that the glassy-rubbery film exhibits the highest sensitivity for detecting organophosphorous vapor. The thicker the glassy and glassy-rubbery film implies a higher sensitivity. Moreover, the SAW vapor sensor based on the rubbery film represents the response of acoustically thick layers which has a peak in attenuation with an increasing vapor adsorption. The selectivity factor between DMMP (10 ppm) and H_2O (40%RH) is so low that the selectivity of FPOL film towards water is ineffecient. However, the selectivity factor between ethanol (10 ppm) and DMMP (10 ppm) is as high as 2512, thus confirming that the selectivity of FPOL film towards ethanol is good. Therefore, a precise and dry humidity control in the sensors system with FPOL coating is required.

1. Introduction

Chemical sensor development is increasingly driven by the need for real-time analyses in industrial process control, environmental monitoring chemical warfare, and biomedical analysis. These applications often use analytical techniques such as gas chromatography (GC), gas chromatography-mass spectrometry (MS), atomic absorption spectrometry, and high performance liquid chromatography. However, these methods require large and expensive instrumentation that have a slow response time and are not mobile. Chemical sensors can be categorized as optical waveguides, devices based on electrical phenomena, and acoustic oscillator devices.

Surface acoustic wave (SAW) devices are attractive for chemical sensor applications owing to their small size, low cost, high sensitivity and reliability. Details regarding SAW devices can be found elsewhere [1, 2], and the feasibility of using SAW structure for vapor detection has been examined as well [3–7]. Most SAW vapor sensors vary the SAW phase velocity and attenuation as the vapor adsorbs in the chemical interface. The chemical interface is chemical or biochemical compounds over the SAW propagating path, and selectively and reversibly interacts with the specific analyte vapor. The shift in phase velocity and attenuation is measured by recording the frequency and insertion loss of SAW devices, respectively. Various effects, including mass loading, viscoelastic (elastic) effect loading, and acousto-electric coupling [8–11], contribute to SAW vapor response.

Modern vapor sensors capable of real-time monitoring of organophosphorous compounds, i.e., a nerve agent, are currently lacking. The development of acoustic sensors for organophosphorous compounds has received considerable attention, with those studies focusing on the feasibility of selecting appropriate chemical interfaces [12–16]. As is well known, polymer films are the primary chemical interfaces for organophosphorous compounds. The polymers have a higher sensitivity, lower detectable limit, and better ability to operate at room temperature than metal-oxide films. Related investigations only discuss how mass loading affects the response of sensors.

This study elucidates the ability of polymer fluoropolyol (FPOL) coated SAW vapor sensors to detect the dimethy methyl phosphonate (DMMP). DMMP is an organophosphorous nerve agent. The mass and viscoelastic effects of the polymer are simulated and studied. Also described herein are the effects of environmental humidity factor and interference vapor.

2. Theory

Fig. 1 illustrates the coordinate system in this study. The SAW propagates at x_1 direction. The complex propagation factor β is represented by both wavenumber k

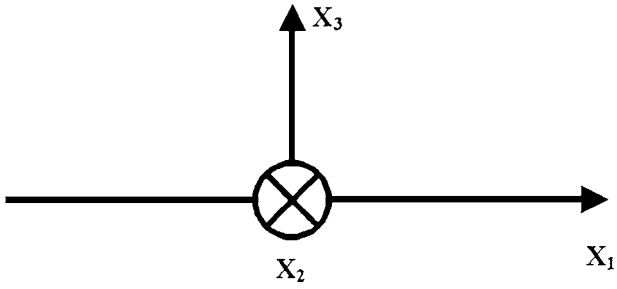

Figure 1 The coordinate system used in this work.

and attenuation α,

$$\beta = k - j\alpha = \frac{\omega}{V} - j\alpha \tag{2}$$

where $j = \sqrt{-1}$, ω is the angular frequency, and V is the phase velocity of SAW. When the frequency is a constant, a change in wave propagation can be represented by

$$\Delta\beta = -k_0 \frac{\Delta V}{V_0} - j\Delta\alpha \tag{3}$$

in a normalized form

$$\frac{\Delta\beta}{k_0} = -\frac{\Delta V}{V_0} - j\frac{\Delta\alpha}{k_0} \tag{4}$$

where k_0 is the unperturbed wavenamber, V_0 is the unperturbed phase velocity of SAW, and $\Delta\beta$, ΔV and $\Delta\alpha$ are the change of β, V and α, respectively. Using Equation 4, the change in complex propagation factor β can be decomposed into the change of the velocity and attenuation. If a SAW device is incorporated in an oscillator loop, the fractional frequency change Δf tracks fractional velocity change, being represented by

$$\frac{\Delta f}{f_0} \cong \frac{\Delta V}{V_0} \tag{5}$$

where f_0 is unperturbed frequency. Loss is represented by the imaginary part of Equation 4

$$Loss = 8.686 \times \frac{\Delta\alpha}{k_0} \tag{6}$$

The change in propagation factor arising from surface mass loading is expressed by

$$\frac{\Delta\beta}{k_0} = -\frac{jV(\nu^* \cdot Z_A \cdot \nu)}{4\omega P} \tag{7}$$

where Z_A is the surface acoustic impedance matrices, ν is the particle velocity matrices, $*$ is the complex conjugate, and P is the power density. The surface acoustic impedance is defined as

$$-T \cdot \hat{x}_3|_{x_3=0} = Z_A \cdot \nu|_{x_3=0} \tag{8}$$

where T is the stress matrix and $\hat{x}_3$ is the unit vector in the x_3 direction. The change of velocity and attenuation is obtained from Equations 4 and 7.

Notably, the elastic properties of viscoelastic materials must be described by a complex modulus when the SAW sensor is coated with a viscoelastic film, such as a polymer film. For example, the shear modulus is represented by $G = G' + jG''$, and the bulk modulus is represented by $K = K' + jK''$. G' and K' are the storage moduli and G'' and K'' are the loss moduli. The Lamé constants (λ and μ) can be expressed by G and K as follows:

$$\begin{aligned} \lambda &= K - \frac{2}{3}G \\ \mu &= G \end{aligned} \tag{9}$$

These parameters are used as variances to alter the polymer characteristics. Based on a previous study [15], the surface acoustic impedance matrix are derived as follows

$$Z_A = \begin{bmatrix} j\dfrac{\gamma_1 G}{\omega}\tan(\gamma_1 h) & 0 & 0 \\ 0 & j\dfrac{\gamma_2 G}{\omega}\tan(\gamma_2 h) & 0 \\ 0 & 0 & j\dfrac{\gamma_3 K}{\omega}\tan(\gamma_3 h) \end{bmatrix}, \tag{10}$$

where

$$\begin{aligned} \gamma_1 &= \omega\sqrt{\frac{1}{G}\left(\rho - \frac{1}{V^2}\cdot\frac{4G(3G+G)}{3K+4G}\right)} \\ \gamma_2 &= \omega\sqrt{\frac{1}{G}\left(\rho - \frac{G}{V^2}\right)} \\ \gamma_3 &= \omega\sqrt{\frac{\rho}{K}} \end{aligned} \tag{11}$$

Substituting Equation 10 with Equation 7, the change of the complex propagation factor can be obtained as

$$\frac{\Delta\beta}{k_0} = \frac{V}{4\omega P}\cdot\left[\frac{\gamma_1 G}{\omega}\tan(\gamma_1 h)\cdot\nu_1^2 + \frac{\gamma_2 G}{\omega}\tan(\gamma_2 h)\cdot\nu_2^2 + \frac{\gamma_3 K}{\omega}\tan(\gamma_3 h)\cdot\nu_3^2\right] \tag{12}$$

For the Rayleigh SAW, the change of the complex propagation factor reduces to

$$\frac{\Delta\beta}{k_0} = \frac{V}{4\omega P}\cdot\left[\frac{\gamma_1 G}{\omega}\tan(\gamma_1 h)\cdot\nu_1^2 + \frac{\gamma_3 K}{\omega}\tan(\gamma_3 h)\cdot\nu_3^2\right] \tag{13}$$

The changes of velocity and attenuation are obtained by substituting Equation 13 with Equation 4.

3. Results and discussion

3.1. Simulation of varying thickness of glassy, glassy-rubbery, and rubbery polymer films

A bulk modulus K and a shear modulus G can be used to specify the mechanical properties of a linear and isotropic polymer. The polymer with a large shear modulus ($G' > 10$ GPa) and $G' \ll G''$ is a glassy (elastic) one. The rubbery (viscoelastic) regime is characterized by $G' \leq 100$ MPa, and G'' is comparable to or less than G'. The glassy-rubbery polymer refers to the polymer with a G' which is 100 MPa $< G' <$ 10 GPa. For the calculations in this section, the operating frequency is considered to be 98 MHz on Y-Z $LiNbO_3$ wafer, and the density of the polymer (FPOL) coating film is 1.65 g/cm^3. Notably, the film thickness is assumed to be less than 0.1 μm since the film thickness in SAW vapor sensors is normally much less than the SAW wavelength λ ($\frac{h_0}{\lambda} < 0.01$). The real part of the bulk modulus is assumed to be a constant [15] so that it equals 10 GPa in this work. From our investigation [17], the influence of the imaginary part of the bulk mudulus can be neglected. For the calculations, the parameter $v_i = \sqrt{P}$ are obtained from Table I. According to this table, the polymer characteristics depend mainly on the real part of the shear modulus [18]. Therefore, G'' can be assumed to be a constant. In Fig. 2, the imaginary part of the shear modulus is assumed to be 50 MPa, and the real part of the shear modulus, G', describing three different polymers is the variable as the film thickness, h_0. The attenuation and velocity shift increase with an increasing film thickness and also increase with a decreasing G'.

3.2. Simulation of vapor sorption by glassy, glassy-rubbery, and rubbery polymer films

The thickness and density of the polymer are taken as a function of the concentration of gas sorbed. The concentration of sorption species C can be expressed as follows:

$$C = \frac{\psi c_V}{M} \tag{14}$$

where ψ is the partition coefficient, c_V is the vapor concentration, and M is the molecular weight of the sorbed vapor. The thickness and density of the polymer film can be expressed by C as follows:

$$\begin{aligned} h(C) &= h_0(1 + CU) \\ \rho(C) &= \frac{\rho_0 + CM}{1 + CU} \end{aligned} \tag{15}$$

TABLE I Properties of YZ-$LiNbO_3$ substrate

Propagation velocity (m/s)	$v_x/\sqrt{P}$	$v_y/\sqrt{P}$ $\times 10^{-6}\sqrt{\omega}[(m/s)/\sqrt{W/m}]$	$v_z/\sqrt{P}$
3488	0	2.625	1.771

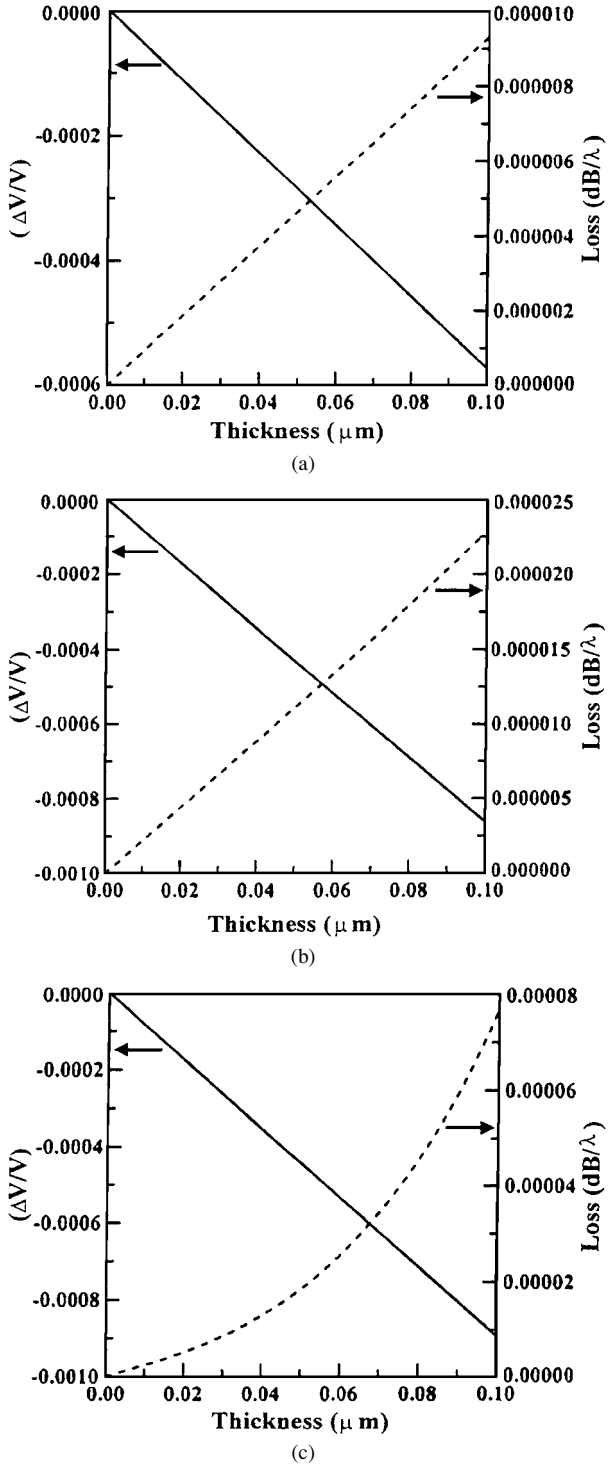

Figure 2 Calculated result of the loss and velocity shift as a function of the film thickness. (a) Glassy, (b) Glassy-Rubbery, (c) Rubbery.

where h_0 and ρ_0 is the thickness and density of the polymer film before vapor sorption, respectively. Also, U is the specific volume of the sorbed vapor obtained from

$$U = \frac{M}{\rho_V} \tag{16}$$

where ρ_V is the density of vapor.

The parameters of DMMP are $\rho_V = 1.145$ g/cm^3, $M = 124$, and $\psi = 10^{6.4}$. The density of FPOL is 1.65 g/cm^3. The operating frequency of Rayleigh-SAW on YZ-$LiNbO_3$ is 98 MHz. In Fig. 3, the imaginary part of shear modulus is assumed to be 50 MPa. The bulk modulus is assumed to be constant, $K' = 10$ GPa

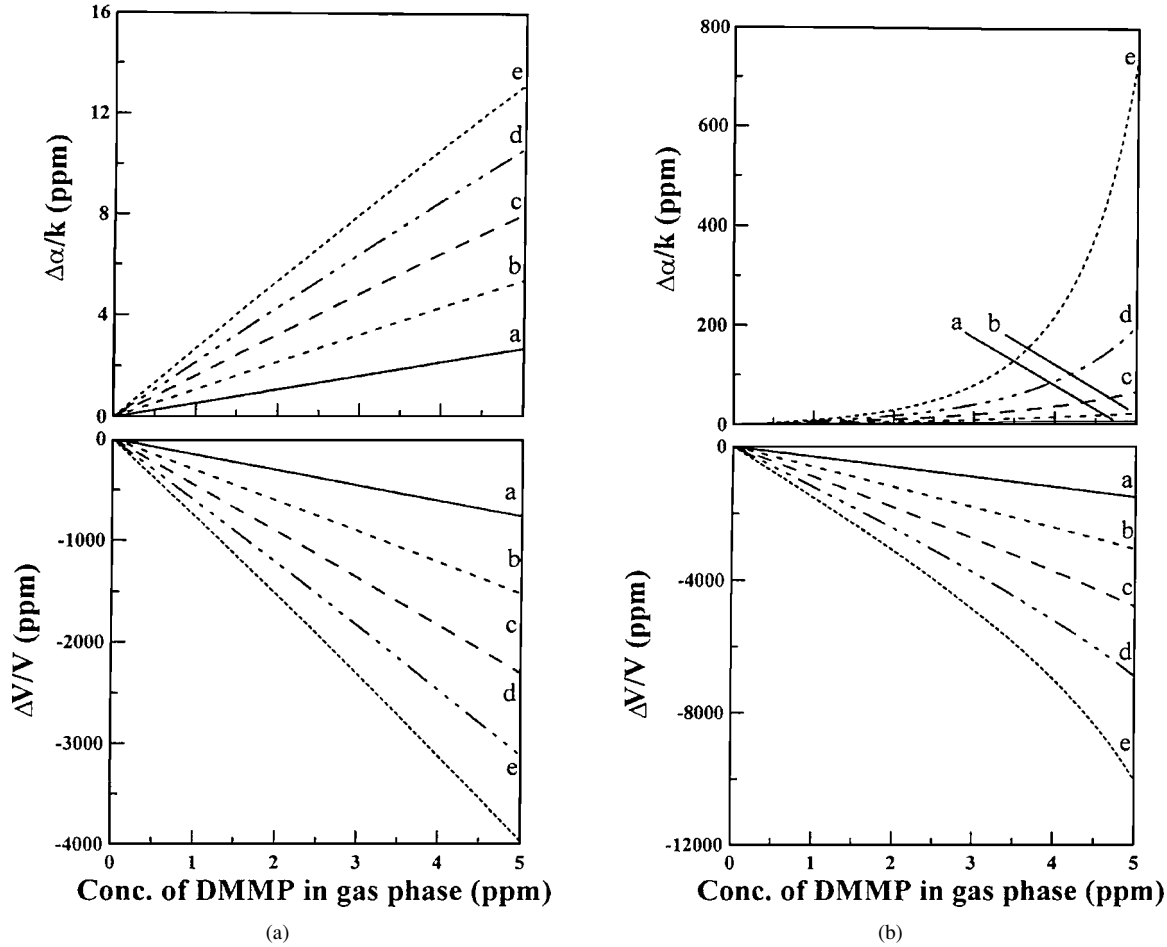

(a) (b)

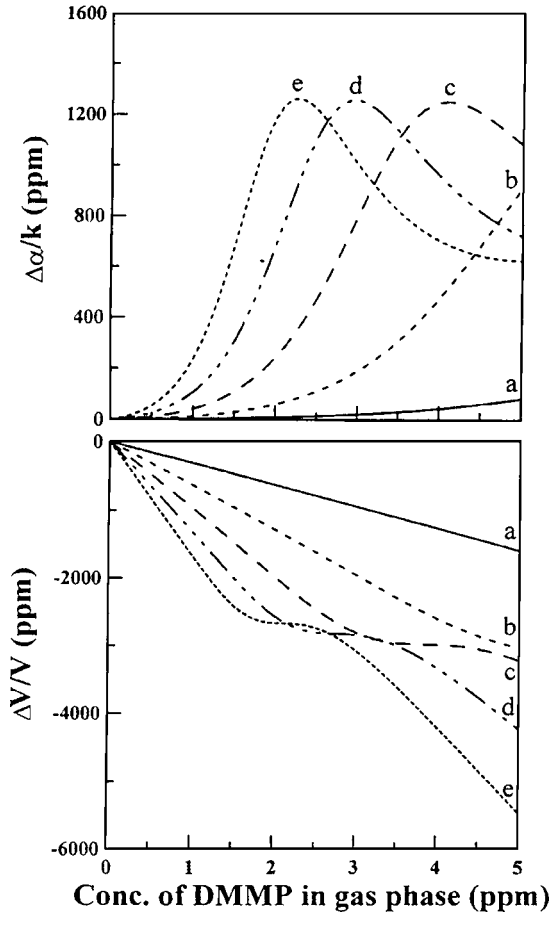

(c)

Figure 3 Calculated results of the attenuation change and velocity shift of Rayleigh-SAW as a function of concentration of DMMP with the film thickness as a parameter. (a) Glassy, (b) Glassy-Rubbery, (c) Rubbery, (a) $h_0 = 0.02$ μm, (b) $h_0 = 0.04$ μm, (c) $h_0 = 0.06$ μm, (d) $h_0 = 0.08$ μm, (e) $h_0 = 0.1$ μm.

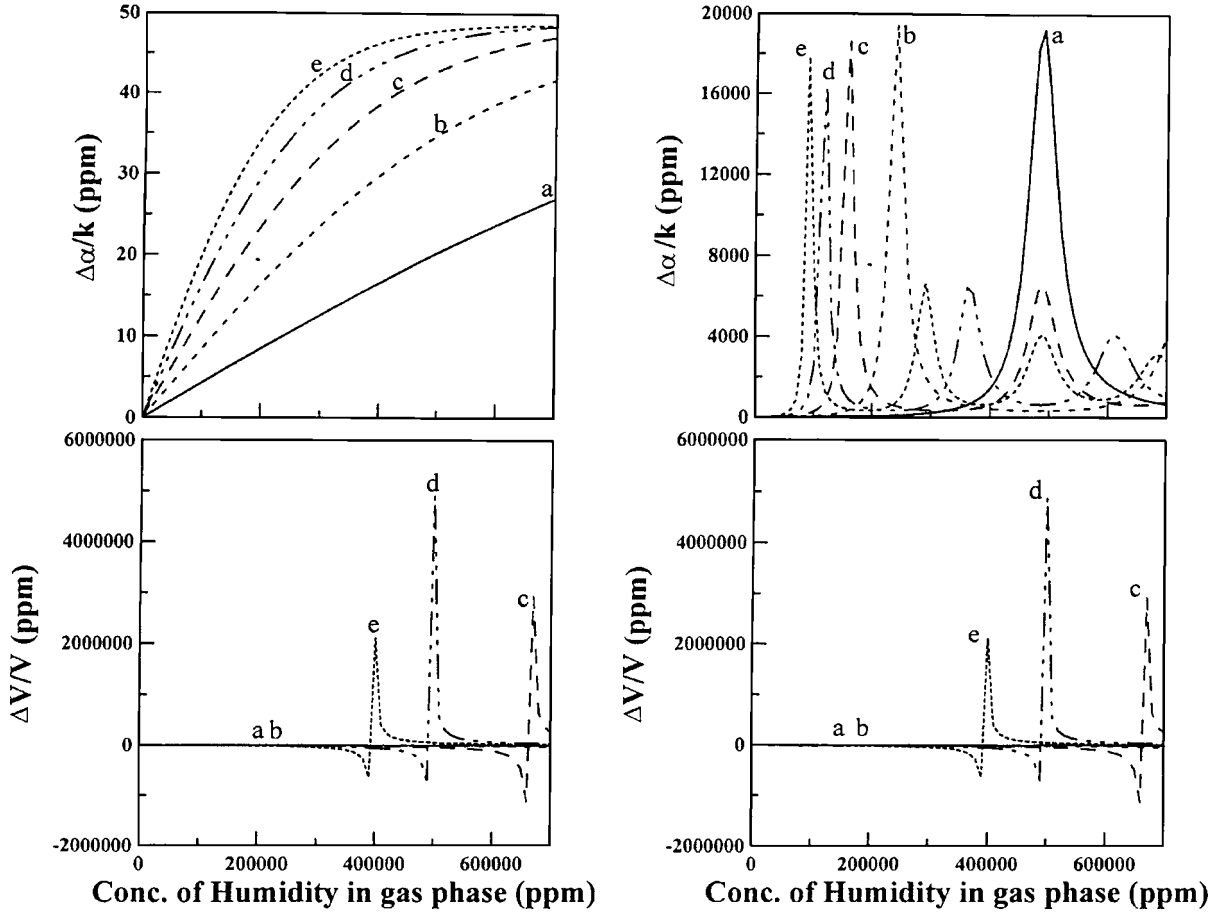

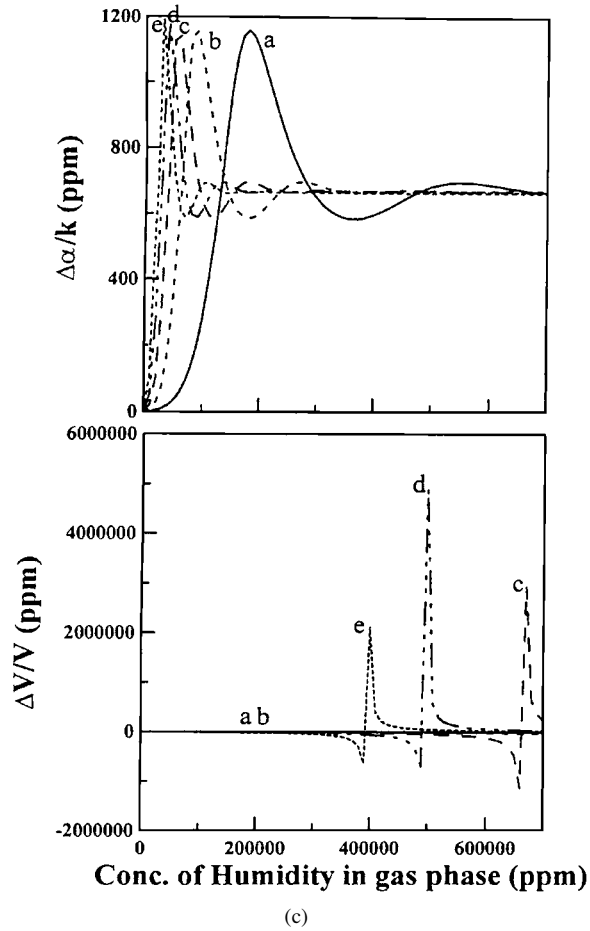

Figure 4 Calculated results of the attenuation change and velocity shift of Rayleigh-SAW as a function of concentration of H_2O with the film thickness as a parameter. (a) Glassy, (b) Glassy-Rubbery, (c) Rubbery, (a) $h_0 = 0.02$ μm, (b) $h_0 = 0.04$ μm, (c) $h_0 = 0.06$ μm, (d) $h_0 = 0.08$ μm, (e) $h_0 = 0.1$ μm.

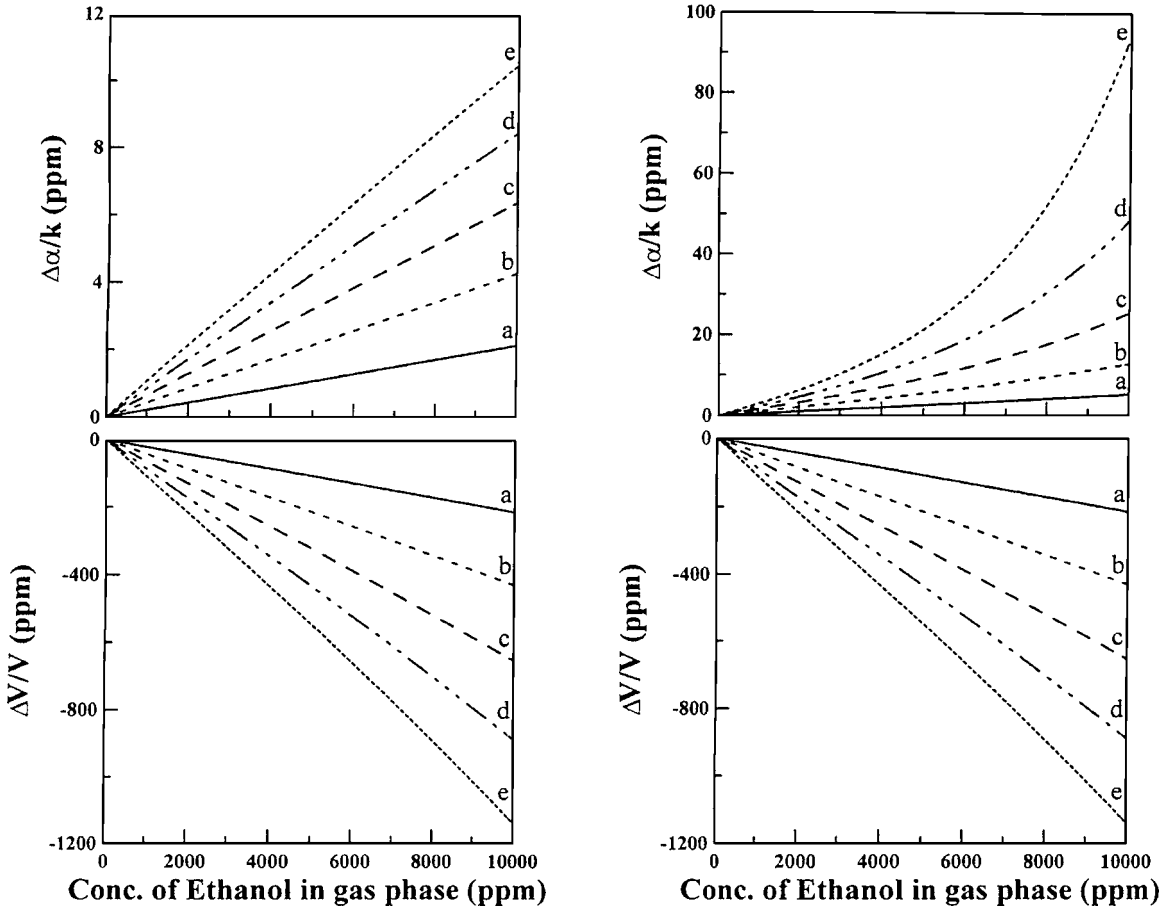

(a) (b)

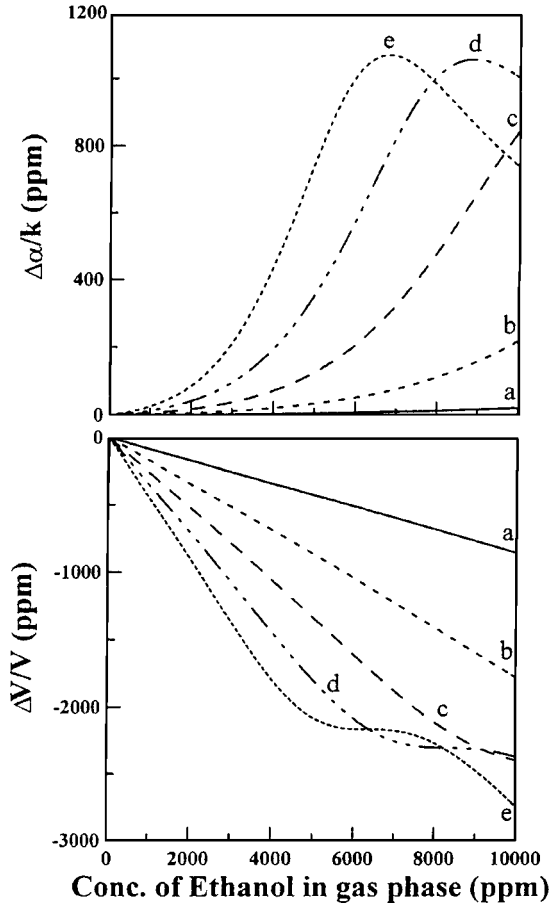

(c)

Figure 5 Calculated results of the attenuation change and velocity shift of Rayleigh-SAW as a function of concentration of Ethanol with the film thickness as a parameter. (a) Glassy, (b) Glassy-Rubbery, (c) Rubbery, (a) $h_0 = 0.02$ μm, (b) $h_0 = 0.04$ μm, (c) $h_0 = 0.06$ μm, (d) $h_0 = 0.08$ μm, (e) $h_0 = 0.1$ μm.

and $K'' = 0$. Fig. 3a and b summarize the effects of glassy and glassy-rubbery polymer. The velocity shift and attenuation increase with an increasing vapor concentration and film thickness. In Fig. 3c, at a high vapor concentration, the plasticization causes the rubbery film to behave as an acoustically thick one. The SAW response of acoustically thick layers has a peak in attenuation with an increasing vapor adsorption. The glassy-rubbery film exhibits a maximum sensitivity as illustrated in Fig. 3. On the other hand, the glassy film is the stiffness material, thereby enhancing the elastic effect. The velocity shift due to elastic effect is opposite to that resulting from mass loading. Hence, the glassy film has a low sensitivity.

3.3. Simulation of environmental humidity factor and ethanol inference vapor with glassy, glassy-rubbery, and rubbery polymer coating

A significant environmental factor for vapor detection is humidity. The parameters of water are $\rho_V = 1.0$ g/cm^3, $M = 18$, and $\psi = 10^{2.3}$. The operating frequency of SAW vapor sensor is 98 MHz in Fig. 4. The imaginary part of shear modulus is assumed to be 50 MPa, and the bulk modulus is assumed to be constant, $K' = 10$ GPa and $K'' = 0$. Fig. 4 summarizes the effect of the environmental humidity factor. The common relative humidity in real environment is 40–70%RH. In Fig. 4, SAW response is evident and sensitive in the range of 40–70%RH. In addition, the sensitivity for water in 40–70%RH is significantly higher than that for DMMP in a few ppm. The selectivity factor, S, can be defined as follows:

$$S = \frac{K_P^A \cdot C_A}{K_P^I \cdot C_I} \tag{17}$$

where K_P^A and K_P^I are air-polymer partition coefficients for analyte and interference vapors, respectively, and C_A and C_I are the concentrations for analyte and interference vapors, respectively. The selectivity factor between DMMP (10 ppm) and H_2O (40%RH) is 0.3, thereby leading to a poor selectivity of FPOL film towards water. Therefore, a precise and dry humidity control in this application is an important requirement. To examine the selectivity towards the interference vapor, ethanol is chosen for simulation. The parameters of ethanol are $\rho_V = 0.78504$ g/cm^3, $M = 46.06952$ and $\psi = 10^{3.0}$. Fig. 5 illustrates the responses for ethanol. These closely resemble the responses for DMMP. The sensitivity for ethanol is markedly less than that for DMMP at the same vapor concentration. By applying Equation 17, the selectivity factor between ethanol (10 ppm) and DMMP (10 ppm) is 2512, thereby ensuring that the selectivity of FPOL film towards ethanol is good.

4. Conclusion

This study examines the feasibility of detecting organophoshporus compounds with SAW sensors based on FPOL polymer. First, the attenuation and velocity shift increase with an increasing film thickness and also increase with a decreasing G' before vapor adsorption. After vapor adsorption, the glassy-rubbery film exhibits a maximum sensitivity. The sensitivity of response increases with an increasing glassy and glassy-rubbery film thickness. The plasticization causes the rubbery film to behave as an acoustically thick one. On the other hand, the glassy film has a strong elastic effect so that the sensitivity of response is low. The selectivity factor between DMMP and H_2O is extremely poor in the common relative humidity of a real environment. Therefore, a precise and dry humidity control for FPOL coating is necessary. Moreover, the selectivity factor between DMMP and ethanol is 2512 so that there is a high selectivity towards ethanol. However, the moduli of the polymer film and the partition coefficient are functions of temperature and an accurate temperature controller for the sensor system is important.

Acknowledgment

The authors would like to thank the National Science Council, R.O.C, for partially supporting this research under Contract No. NSC 88-2213-E-214-029.

References

1. M. S. NIEUWENHUIZEN and A. VENEMA, *Sensors Material* **1** (1989) 261.
2. C. G. FOX and J. F. ALDER, *Analyst* **114** (1989) 997.
3. A. VENEMA, E. NIEUWKOOP, A. W. BARENDSZ and M. S. NIEUWENHUIZEN, *Sensors and Actuators* **11** (1987) 45.
4. M. S. NIEUWENHUIZEN and A. J. NEDERL, *ibid. B* **2** (1990) 97.
5. M. S. NIEUWENHUIZEN and L. L. N. HARTEVELD, *ibid.* **40** (1997) 167.
6. N. M. TASHTOUCH, J. D. N. CHEEKE and N. EDDY, *ibid.* **49** (1998) 218.
7. M. FANG, K. VETELINO, M. ROTHERY, J. HINES and G. C. FRYE, *ibid.* **56** (1999) 155.
8. A. J. RICCO and S. J. MARTIN, *Thin Solid Films* **206** (1991) 94.
9. V. I. ANSIMKIN, I. M. KOTELYANSKII, V. I. FEDOSOV, C. CALIENDO, P. VERATDI and R. VERONA, in *Proc. IEEE Ultrason. Symp.* (1995) p. 515.
10. *Idem.*, in *Proc. IEEE Ultrason. Symp.* (1996) p. 293.
11. M. PENZA, E. MILELLA and V. I. ANSIMKIN, *IEEE Trans. Ultrason. Ferroelect., Freq. Contr.* **45** (1998) 1125.
12. S. J. MARTIN, G. C. FRYE and S. D. SENTURIA, *Anal. Chem.* **66** (1994) 2201.
13. A. J. RICCO and S. J. MARTIN, *Thin Solid Films* **206** (1991) 94.
14. J. GRATE, M. KLUSTY, R. A. McGILL, M. H. ABRAHAM, G. WHITING and J. ANDONIAN-HAFTVAN, *Anal. Chem.* **64** (1992) 610.
15. J. KONDOH, S. SHIOKAWA, M. RAPP and S. STIER, *Jpn, J, Appl. Phys.* **37** (1998) 2842.
16. R. A. McGILL, M. H. ABRAHAM and J. W. GRATE, *American Chemical Society* (1994) 27.
17. C. Y. SHEN, Y. T. SHEN and L. WU, *J. Mater. Sci.*, submitted.
18. D. S. BALLANTINE *et al.*, "Acoustic Wave Sensors" (New York, NY, Academic Press, 1997) p. 92.

Received 11 January
and accepted 1 October 2001